Lithium chloride modulates chondrocyte primary cilia and inhibits Hedgehog signaling

Clare L. Thompson,*[,1] Anna Wiles,[†] C. Anthony Poole,[†] and Martin M. Knight*

*Institute of Bioengineering, School of Engineering and Materials Science, Queen Mary University of London, London, United Kingdom; and [†]Dunedin School of Medicine, University of Otago, Dunedin, New Zealand

ABSTRACT Lithium chloride (LiCl) exhibits significant therapeutic potential as a treatment for osteoarthritis. Hedgehog signaling is activated in osteoarthritis, where it promotes chondrocyte hypertrophy and cartilage matrix catabolism. Hedgehog signaling requires the primary cilium such that maintenance of this compartment is essential for pathway activity. Here we report that LiCl (50 mM) inhibits Hedgehog signaling in bovine articular chondrocytes such that the induction of *GLI1* and *PTCH1* expression is reduced by 71 and 55%, respectively. Pathway inhibition is associated with a 97% increase in primary cilia length from 2.09 ± 0.7 μm in untreated cells to 4.06 ± 0.9 μm in LiCl-treated cells. We show that cilia elongation disrupts trafficking within the axoneme with a 38% reduction in Arl13b ciliary localization at the distal region of the cilium, consistent with the role of Arl13b in modulating Hedgehog signaling. In addition, we demonstrate similar increases in cilia length in human chondrocytes *in vitro* and after administration of dietary lithium to Wistar rats *in vivo*. Our data provide new insights into the effects of LiCl on chondrocyte primary cilia and Hedgehog signaling and shows for the first time that pharmaceutical targeting of the primary cilium may have therapeutic benefits in the treatment of osteoarthritis.—Thompson, C. L., Wiles, A., Poole, C. A., Knight, M. M. Lithium chloride modulates chondrocyte primary cilia and inhibits Hedgehog signaling. *FASEB J.* 30, 000–000 (2016). www.fasebj.org

Key Words: *cilia length · osteoarthritis · Arl13b*

Lithium chloride, a drug previously used for the treatment of bipolar disorder (1–3), has recently been shown to exhibit significant therapeutic potential as a treatment for arthritis (4, 5). These studies show that LiCl inhibits cartilage degradation *in vitro* in response to the inflammatory cytokine IL-1. LiCl disrupts the downstream activation of p38 MAPK and nuclear factor κ-light-chain-enhancer of activated B cells (NF-κB) in response to IL-1, thus inhibiting the induction of catabolic enzymes such as A disintegrin and metalloproteinase with thrombospondin motifs 5 and matrix metalloproteinases 3 and 13. Consequently, this inhibits cartilage degradation (4, 5) and loss of cartilage mechanical properties (6). Similar findings have been reported *in vivo* wherein both dietary and intra-articular

injection of LiCl were found to reduce the severity of cartilage damage in surgical models of osteoarthritis (OA) (5).

Recent studies have shown that LiCl inhibits Hedgehog signaling in pancreatic ductal adenocarcinoma cells (7). Several studies have now implicated Hedgehog signaling in the development and progression of OA (8–12). The expression of Indian hedgehog (Ihh) is increased in early cartilage lesions (8, 12), and the concentration of Ihh in the synovial fluid increases with the severity of cartilage damage in human knee joint OA (11, 12). Consequently, Hedgehog signaling is activated in osteoarthritic cartilage, where it promotes chondrocyte hypertrophy and matrix catabolism (10, 11). In mouse models, pharmacologic inhibition of the Hedgehog pathway reduces the severity of surgically induced OA (10). More recent studies have reported that inducible, cartilage-specific deletion of Ihh also prevents disease progression, highlighting the importance of ligand-mediated signaling in this disease (9).

LiCl has been shown to affect the primary cilium, a dedicated signaling compartment at the cell surface (13–16). The primary cilium is rapidly becoming recognized as an important player in arthritis as a result of its established roles in Wnt (17, 18) and Hedgehog signaling (19), and more recently in its involvement in chondrocyte mechanotransduction (20–22). The cilium comprises a modified centriole called the basal body from which extends a microtubule-based scaffold, the ciliary axoneme. The axoneme is surrounded by a distinct membrane, which can become specialized in a cell-type-specific manner. A gated diffusion barrier exists at the ciliary base, and thus the entry and exit of proteins into the ciliary axoneme is tightly regulated (23, 24). Soluble proteins and transmembrane receptors are conducted along ciliary microtubules by a process called intraflagellar transport (IFT) (25, 26). The anterograde motor kinesin 2 is responsible for the transport of IFT cargo, like tubulin, from the base of the cilium to the distal tip, while cytoplasmic dynein 2 mediates retrograde transport from the tip to base (27, 28). Cilia assembly and disassembly is initiated at the distal tip; IFT is thus essential to maintain the size of the ciliary compartment (29). Studies have shown that LiCl promotes significant elongation of the ciliary axoneme in fibroblasts (14, 15) and neuronal

---

[1] Correspondence: School of Engineering and Materials Science, Queen Mary University of London, London E1 4NS, United Kingdom. E-mail: clare.l.thompson@qmul.ac.uk

cells (13); however, the consequences of this elongation for cilia-mediated signaling pathways has not been explored.

The coordinated transport of Hedgehog signaling components through the ciliary compartment is essential for pathway activation. The Hedgehog receptor Patched (Ptch1) is localized to the ciliary membrane in the absence of ligand. Upon ligand binding, Ptch1 exits the cilium and triggers the ciliary accumulation of a second transmembrane protein, Smoothened (Smo), a process that is mediated by a number of proteins such as the small GTPase Arl13b (30, 31). Within the cilium, Smo regulates the activity of the Gli transcription factors (Gli2 and Gli3), the downstream effectors in this pathway (32). These transcription factors are constitutively expressed and accumulate at the ciliary tip in response to ligand; once activated, they translocate to the nucleus where they regulate gene transcription (19, 33, 34). At the nucleus, their function is further amplified by the induction of a third transcription factor, Gli1. Gli1 has also been shown to up-regulate Ptch1 expression, thereby establishing a negative-feedback mechanism (35). The measurement of both *GLI1* and *PTCH1* mRNA can be used to monitor pathway activity. The size, frequency, and velocity of IFT particles within the cilium are influenced by cilia length (36). This affects the delivery of cargo to the ciliary tip such that longer cilia have a reduced level of protein entry, which undoubtedly influences cilia-mediated signaling (37, 38). Indeed, Cruz *et al.* (39) report that during embryonic development, Foxj1 mediated lengthening of primary cilia in the neural tube attenuates Hedgehog signaling to regulate cellular identity and formation of the embryonic floor plate.

In the current study, we hypothesized that LiCl influences chondrocyte Hedgehog signaling and that this is achieved through its effects on primary cilia structure. We demonstrated that LiCl treatment results in the inhibition of ligand-mediated Hedgehog signaling. LiCl treatment results in rapid cilia axoneme growth in isolated bovine chondrocytes, which correlates with Hedgehog pathway inhibition and is associated with reorganization of the ciliary compartment and disruption of Arl13b ciliary localization. Furthermore, we report that LiCl induces cilia elongation in human articular chondrocytes *in vitro* and *in vivo* using a rat model designed to mimic long-term lithium treatment in human patients. Thus, we show for the first time that LiCl suppresses Hedgehog signaling through alterations in primary cilia structure.

MATERIALS AND METHODS

Cell isolation and culture

For bovine articular chondrocytes, full-depth slices of articular cartilage were removed from the proximal surface of the bovine metacarpal phalangeal joint and primary articular chondrocytes isolated by enzymatic digestion, as previously described (40). Chondrocytes were cultured in DMEM supplemented with 10% (v/v) fetal calf serum, 1.9 mM L-glutamine, 96 U/mL penicillin, 96 µg/ml streptomycin, 19 mM 2-[4-(2-hydroxyethyl)piperazin-1-yl]ethanesulfonic acid (HEPES) buffer, and 0.74 mM L-ascorbic acid (all Sigma-Aldrich, Poole, United Kingdom) at 37°C and 5% CO_2, and used in experiments at P0.

Human articular chondrocytes were obtained commercially (Articular Engineering, Northbrook, IL, USA). Cells were isolated from full-depth cartilage slices removed from the femoral condyles of male cadaver donors aged 60 to 71 yr. Chondrocytes were cultured in chondrocyte culture medium (Articular Engineering) at 37°C and 5% CO_2 and used in experiments from P0 to P3.

For experiments, articular chondrocytes were seeded onto serum-coated glass coverslips or plastic tissue culture plates. Upon reaching confluence, cells were treated with 0 to 50 mM LiCl (Sigma-Aldrich) for up to 24 h in the presence or absence of 1 µg/ml recombinant Indian hedgehog (r-Ihh; R&D Systems, Minneapolis, MN, USA). At the end of the experiment, cell viability was assessed by calcein AM/ethidium homodimer (Life Technologies, Carlsbad, CA, USA) labeling and fluorescence microscopy, and separate samples were processed for immunofluorescence, Western blot analysis, and real-time PCR.

Animal studies

Male Wistar rats (3 per treatment group) were used to examine the influence of dietary lithium on primary cilia length *in vivo*. Tissue was obtained from rats fed a lithium-enriched diet, 60 mmol lithium/100 g ground rat food, for 9 mo. Rats were initially given food containing 40 mmol lithium for the first 7 d, followed by 9 mo at the higher dose, enabling them to make physiologic adjustments to the treatment regimen. This is equivalent to approximately 20 yr of treatment in human patients, and it resulted in plasma lithium levels comparable to therapeutic levels in human plasma (0.8–1.3 mM). Plasma lithium levels were monitored through a blood sample taken from the tail vein at the end of the experimental period. Age-matched controls were kept on normal food and water. To minimize the lack of weight gain associated with lithium-induced diuresis, rats were given continuous access to a salt block and free access to water. These studies were approved by the Otago University animal ethics committee (AEC 98/10).

Antibodies

Mouse anti-acetylated tubulin, clone 611B-1 (1:2000; Sigma-Aldrich), and rabbit anti-Arl13b (1:2000; Proteintech, Manchester, United Kingdom) were used for the detection of the ciliary axoneme in isolated cells. Mouse anti-acetylated tubulin, clone C3B9 (41), was used for the detection of primary cilia in tissue. For Western blot analysis, rabbit anti–β-catenin ser675 (1:200; Cell Signaling Technology, Danvers, MA, USA), rabbit anti-tubulin (1:1000; Sigma-Aldrich), mouse anti-actin (1:5000; Abcam, Cambridge, MA, USA), and mouse anti-acetylated tubulin, clone 611B-1 (1:500; Sigma-Aldrich) were used.

Immunofluorescence confocal and super resolution microscopy

For isolated cells, coverslips were fixed with 4% paraformaldehyde for 10 min. Fixation was followed by detergent permeabilization with 0.5% Triton X-100 and blocking with 5% serum for 1 h. Samples were incubated with primary antibodies at 4°C overnight. After repeated washing in 0.1% bovine serum albumin/PBS, cells were incubated with appropriate Alexa Fluor–conjugated secondary antibodies (1:1000; Life Technologies) for 1 h at room temperature and nuclei were detected with 1 µg/ml DAPI. After repeated washing in 0.1% bovine serum albumin/PBS, coverslips were mounted with Prolong gold reagent (Life Technologies).

For immunohistochemical staining of primary cilia, cartilage samples were fixed in 10% neutral buffered formalin for 48 h,

decalcified in 10% EDTA pH 7 0 to 7.2, and embedded in paraffin wax. Sections 20 μm thick were cut perpendicular to the surface of the cartilage; paraffin was then removed and samples were processed as above for the detection of primary cilia.

For primary cilia length measurement, samples were imaged using a Leica TCS SP2 confocal microscope with a ×63, 1.3 NA lens. Confocal Z stacks were generated throughout the entire cellular profile using a Z step size of 0.5 μm, ×2 zoom, and an image format of 1024 × 1024 pixels. This produced an xy pixel size of 0.116 × 0.116 μm. Z stacks were reconstructed and an xy maximum intensity projection used for the measurement of cilia length using ImageJ software (Image Processing and Analysis in Java; U.S. National Institutes of Health, Bethesda, MD, USA). The length of approximately 100 cilia was measured over 5 representative fields of view for each condition per experiment. For primary cilia prevalence and Ki-67 staining, samples were imaged using a Leica DMI4000B epifluorescent microscope with a ×63/1.4 NA objective. The proportion of ciliated/Ki-67–positive cells was determined in 10 representative fields of view for each condition per experiment. For structural illumination microscopy, samples were imaged on a Zeiss 710 ELYRA PS.1 microscope with a ×63/1.4 NA objective.

Western blot analysis

Cells were lysed in NP-40 buffer (1% NP-40, 150 mM NaCl, 50 mM Tris pH 8.0) containing 50 mM NaVO$_4$ and protease inhibitor cocktail (Roche, Basel, Switzerland). The lysate was homogenized and centrifuged at 13,000 rpm for 15 min. The supernatant was collected and protein concentration determined by bicinchoninic acid assay. SDS-PAGE was performed using 40 μg total protein and run on 5–20% gradient gels (Bio-Rad, Hercules, CA, USA). Proteins were transferred to a nitrocellulose membranes and blocked for 1 h at room temperature in 5% nonfat milk or 5% bovine serum albumin in Tris-buffered saline according to the manufacturer's recommendations, then incubated with primary antibodies at 4°C overnight. Membranes were washed and then incubated with appropriate infrared secondary antibodies (Li-Cor Biosciences, Lincoln, NE, USA) for 1 h at room temperature. Membranes were washed again and visualized using the Li-Cor Odyssey. Analysis of band intensity was performed by Li-Cor software.

RNA extraction, cDNA synthesis, and real-time PCR

Total RNA was isolated from individual wells using an RNeasy Kit (Qiagen, Germantown, MD, USA) and converted to cDNA using the Quantitect reverse transcription kit (Qiagen) according to the manufacturer's instructions. For real-time PCR, reactions were performed in 10 μl volumes containing 1 μl cDNA (diluted 1:2), 5 μl Kapa SYBR Fast Universal 2× qPCR Master Mix (Kapa Biosystems, London, United Kingdom) containing SYBER green dye, 0.2 μl ROX reference dye, and 1 μl optimized primer pairs (**Table 1**). An annealing temperature of 60°C was used for all PCR reactions. Fluorescence data was collected using the MX3000P qPCR instrument (Stratagene) and analyzed using the relative standard curve method (42).

The expression of *GLI1* and *PTCH1* were monitored as a measure of Hedgehog pathway activity and normalized to the expression of 18S ribosomal RNA, which was not significantly altered by the experimental conditions used in this study.

Statistical analyses

All statistical analyses were conducted by Graph Pad Prism 6.01 (GraphPad, La Jolla, CA, USA). *N* refers to the number of donors

TABLE 1. *Primer sequences*

Gene	Species	Sequence, 5'–3'
PTCH1	Bovine	F - ATGTCTCGCACATCAACTGG
		R - TCGTGGTAAAGGAAAGCACC
GLI1	Bovine	F - ACCCCACCACCAGTCAGTAG
		R - TGTCCGACAGAGGTGAGATG
18S RNA	Bovine	F - GCAATTATTCCCCATGAACG
		R - GGCCTCACTAAACCATCCAA

(independent experiments) and *n* refers to the number of technical replicates analyzed per experimental group. Data are presented as means ± SD, except for cilia length, for which median values are described. Before analyses, data sets that failed normality testing (Shapiro-Wilk test) were converted to a Gaussian distribution by Box-Cox transformation. Thereafter, all data were analyzed by 1- or 2-way ANOVA and as indicated in the figure legends with *post hoc* Tukey's multiple comparisons. Differences were considered statistically significant at $P \leq 0.05$.

RESULTS

Ligand-dependent Hedgehog signaling is inhibited by LiCl

After 24 h r-Ihh treatment, real-time PCR analysis showed that the mRNA levels of *GLI1* (**Fig. 1A**) and *PTCH1* (Fig. 1B) were significantly increased by 4.48- and 3.16-fold, respectively. LiCl treatment alone did not significantly affect gene expression. However, dose-dependent inhibition of *GLI1* and *PTCH1* (r^2 = 0.8685 and 0.9043, respectively; Supplemental Fig. S1) induction in response to r-Ihh was observed such that Hedgehog pathway activation was not significantly activated in the presence of 50 mM LiCl (Fig. 1A, B). Chondrocyte viability was maintained throughout the experimental period, and effects on cell cycle status were minimal (Supplemental Fig. S2). These data indicate that LiCl inhibits ligand-dependent Hedgehog signaling in bovine articular chondrocytes.

Hedgehog pathway inhibition is independent of glycogen synthase kinase

LiCl functions primarily as a glycogen synthase kinase (GSK) inhibitor, the blockade of which results in the accumulation of β-catenin and activation of canonical Wnt signaling (43). After 24 h LiCl treatment, Western blot analysis revealed that the level of activated β-catenin was not significantly altered (Fig. 1C, D), suggesting that LiCl does not influence Hedgehog signaling through GSK inhibition and canonical Wnt signaling. Indeed, the induction of *GLI1* and *PTCH1* in response to r-Ihh was not significantly different in the presence of the GSK inhibitor CHIR-99021 (Supplemental Fig. S3).

Primary cilia elongation occurs in response to LiCl

A functioning primary cilium is required for ligand-dependent Hedgehog signaling (44–46). Previous studies

Figure 1. Ligand-dependent Hedgehog signaling is inhibited by LiCl. Bovine articular chondrocytes treated with 0–50 mM LiCl ± r-Ihh for 24 h. Real-time PCR for *GLI1* (*A*) and *PTCH1* (*B*) gene expression. Data are expressed as fold change relative to 0 mM LiCl control (*N* = 3, *n* = 9). *C*) Representative Western blot for activated β-catenin; β-actin was used as loading control. *D*) Quantification of band intensity for β-catenin Western blot analysis; β-catenin is expressed relative to β-actin (*N* = 3, *n* = 3). Statistical analysis performed by 2-way and 1-way ANOVA, respectively, with Tukey's multiple comparisons test. Statistically significant differences between control and r-Ihh-treated groups is indicated at **$P < 0.01$ and ***$P < 0.001$, and differences relative to r-Ihh treated control (0 mM LiCl) are indicated at $^{\$}P < 0.05$) and $^{\$\$\$}P < 0.001$.
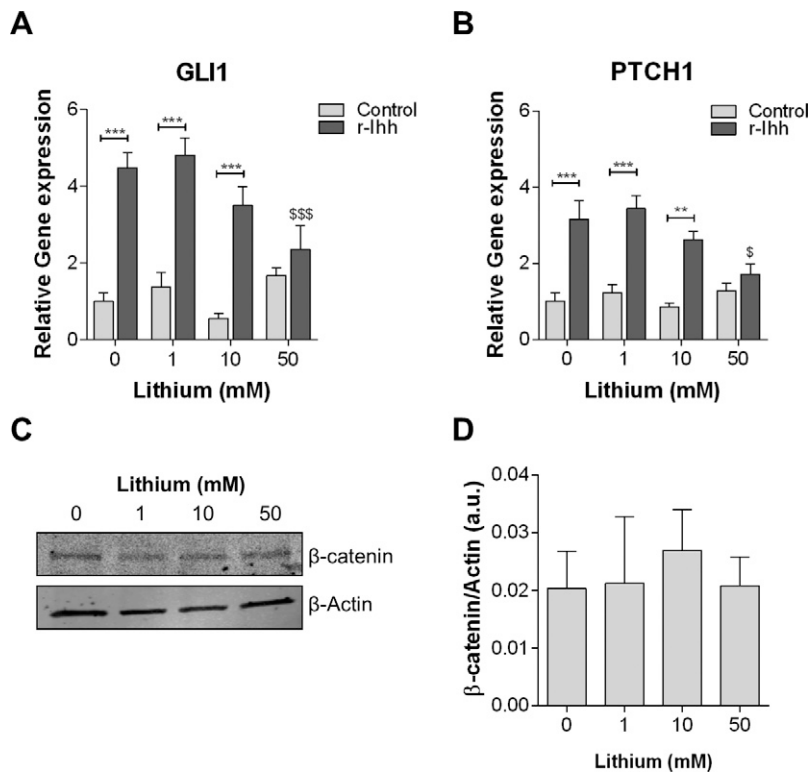
have shown that LiCl influences primary cilia length in numerous cell types (13, 47). After 24 h LiCl treatment, immunocytochemistry was performed and the chondrocyte primary cilium labeled with 2 ciliary markers, acetylated α-tubulin and Arl13b (**Fig. 2***A*). While the proportion of ciliated cells was not significantly influenced by LiCl treatment (Fig. 2*B*), a dose-dependent increase in axoneme length was observed (r^2 = 0.9975, Supplemental Fig. S1 and Fig. 2*C*). Cilia length was maximally increased from 2.09 ± 0.7 to 4.06 ± 0.9 μm at 50 mM LiCl, coinciding with maximum pathway inhibition (Figs. 1*A, B* and 2*C*).

The effects of 50 mM NaCl and KCl on cilia prevalence (Fig. 2*D*) and length (Fig. 2*E*) were also examined. Alterations in cilia length were observed with KCl only; however, these were significantly less pronounced, suggesting that dramatic elongation is specific to LiCl (Fig. 2*D*).

Primary cilia elongation is independent of GSK

Nakakura *et al.* (14) reported that in fibroblasts, LiCl-mediated inhibition of GSK releases an inhibitory block on the enzyme α-tubulin acetyl transferase 1, causing a dramatic increase in whole-cell acetylated tubulin levels and an increase in cilia length. Immunocytochemistry revealed that the distribution of acetylated tubulin was altered in chondrocytes treated with 50 mM LiCl (**Fig. 3***A*) such that staining was increased at the ciliary base (Fig. 3*A*, inset). However, no significant differences in the total levels of tubulin acetylation were identified by Western blot analysis (Fig. 3*B, C*). Moreover, the GSK inhibitor CHIR-99021 did not significantly influence cilia prevalence or length (Fig. 3*D–F*), suggesting that

cilia elongation occurs through an alternative mechanism in articular chondrocytes.
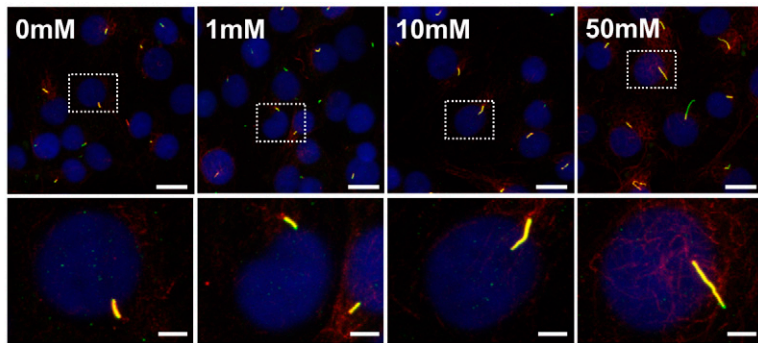
Primary cilia elongation is rapid, occurring in 1 h of LiCl treatment

The temporal effects of LiCl on cilia length were analyzed over 1 to 24 h. In control cells, cilia length did not vary significantly over the 24 h period (Supplemental Fig. S4). In response to LiCl, cilia length was significantly increased after 1 h at all doses (**Fig. 4**). At 1 mM LiCl, cilia length was increased at 1 and 3 h; however, this response was not maintained over 24 h (Fig. 4*A*). In contrast, maximal cilia elongation was achieved at 1 h in response to 10 mM LiCl and was maintained throughout the culture period (Fig. 4*B*). At 50 mM LiCl, the axoneme continued to grow after 1 h, but at a slower rate, reaching a median length of 4.06 ± 0.9 μm by 24 h (Fig. 4*C*). These data indicate that ciliary elongation *in vitro* is rapid, but transient at low doses.
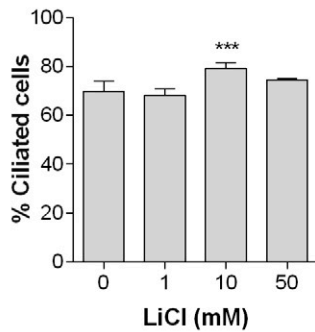
LiCl-induced cilia elongation is associated with reorganization of ciliary compartment

Arl13b, a ciliary protein within the ADP-ribosylation factor family and Ras superfamily of GTPases, has been implicated in the dynamic localization of Hedgehog signaling components to the ciliary compartment in response to ligand stimulation (30). After 1 h LiCl treatment, the proportion of primary cilia exhibiting accumulations of Arl13b at their distal tip was increased, giving the appearance of a swollen or bulbous tip (r^2 = 0.5509, **Fig. 5***A* and Supplemental Fig. S1). In response
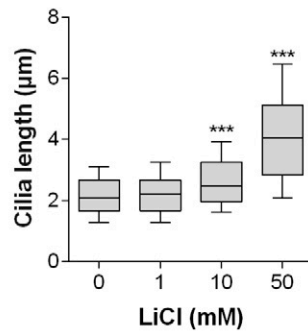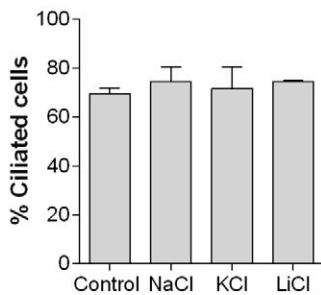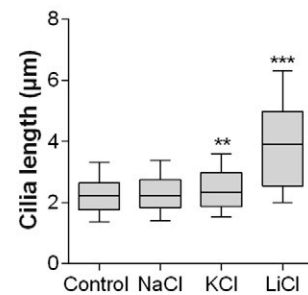
Figure 2. Primary cilia elongation occurs in response to LiCl. *A)* Confocal immunofluorescence of bovine articular chondrocytes treated for 24 h with 0 to 50 mM LiCl. Scale bars, 20 μm. White boxes indicate enlarged representative cells shown under each condition. Scale bar, 5 μm. Primary cilia were labeled for acetylated α-tubulin (red) and arl13b (green); nuclei were counterstained with DAPI (blue). Primary cilia prevalence ($N = 3$, $n = 30$ fields) (*B*) and primary cilia length ($N = 3$, $n \geq 200$ cilia per group) (*C*) at 24 h. Primary cilia prevalence ($N = 3$, $n = 30$ fields) (*D*) and primary cilia length ($N = 3$, $n \geq 200$ cilia per group) (*E*) after 50 mM NaCl or KCl treatment for 24 h. For box-and-whisker plots, line is median, box 25th to 75th percentile with 10th to 90th percentile whiskers. Statistical analysis performed by 2-way ANOVA with Tukey's multiple comparisons tests. Statistically significant differences relative to untreated control are indicated at **$P < 0.01$ and ***$P < 0.001$.

to 50 mM LiCl 15.3 ± 8.6% of cells exhibited bulbous tips compared with just 4.5 ± 0.81% in untreated cells (Fig. 5*B*). After 24 h, the proportion of cilia with swollen tips had returned to the level of the control (data not shown). These tip structures were observable using structural illumination microscopy, which also highlights the membrane localization of this protein, which becomes increasingly patchy and disrupted along the length of the axoneme as cilia elongate (Fig. 5*C*). The presence of bulbous tips is generally associated with defects in retrograde IFT; thus, these data are consistent with a dose-dependent imbalance in the molecular transport mechanisms regulating cilia length (48, 49).

To examine the effects of LiCl on Arl13b trafficking, intensity measurements were taken along the length of the axoneme. At 1 h, the Arl13b intensity profile appeared relatively uniform in control cells and cells treated with 50 mM LiCl (Fig. 5*D, E*). Moreover, mean Arl13b intensity was not significantly different between the 2 groups (Fig. 5*I*). In contrast, while the Arl13b intensity profile remained relatively uniform in control cilia at 24 h

(Fig. 5*F*), in cells treated with 50 mM LiCl Arl13b, intensity appeared weaker toward the distal tip (Fig. 5*G*), and mean Arl13b intensity was significantly reduced in these cilia (Fig. 5*J*). Division of the cilium into proximal and distal regions confirmed that this was largely due to a reduction in the distal region at 24 h (Fig. 5*I, K*).

At both 1 and 24 h, total Arl13b staining within the axoneme was increased, suggestive of an increase in ciliary trafficking. However, while at 1 h the amount of Arl13b per micrometer of axoneme remained constant between control and treated cilia, at 24 h this was significantly reduced, thus highlighting the possibility that a threshold length exists at which the Arl13b trafficking equilibrium can be maintained.

LiCl induces primary cilia elongation in isolated human chondrocytes and *in vivo* in rat chondrocytes

After 24 h treatment with 50 mM LiCl, primary cilia length was significantly increased in isolated human articular chondrocytes (**Fig. 6*A, B***), suggesting that this
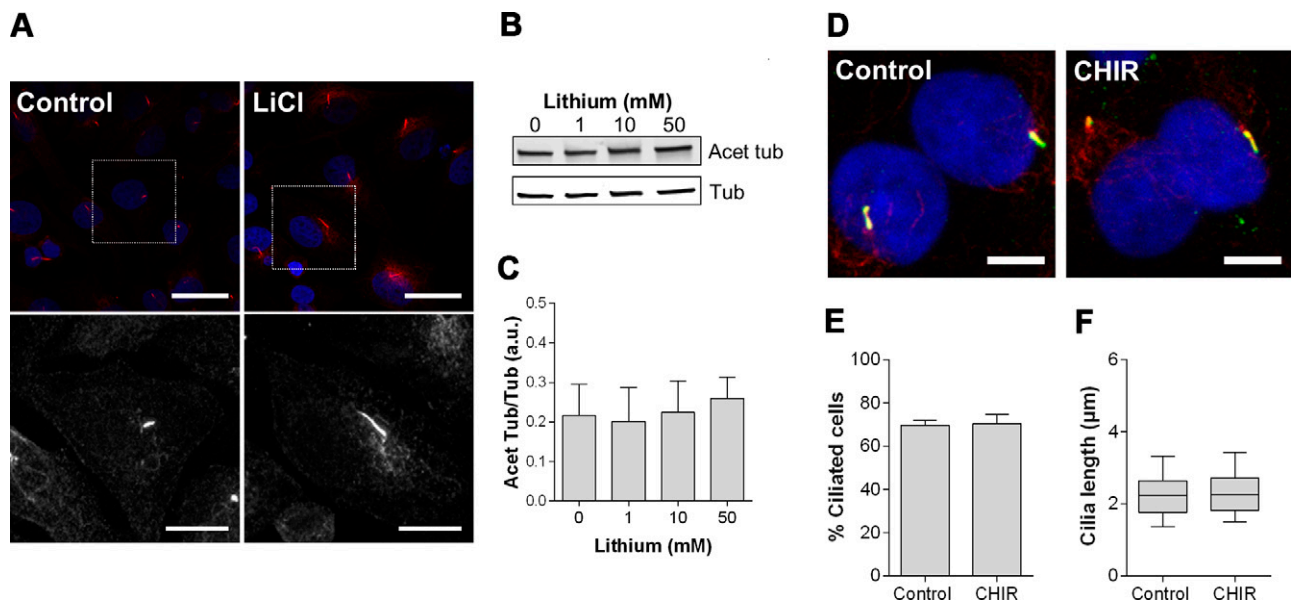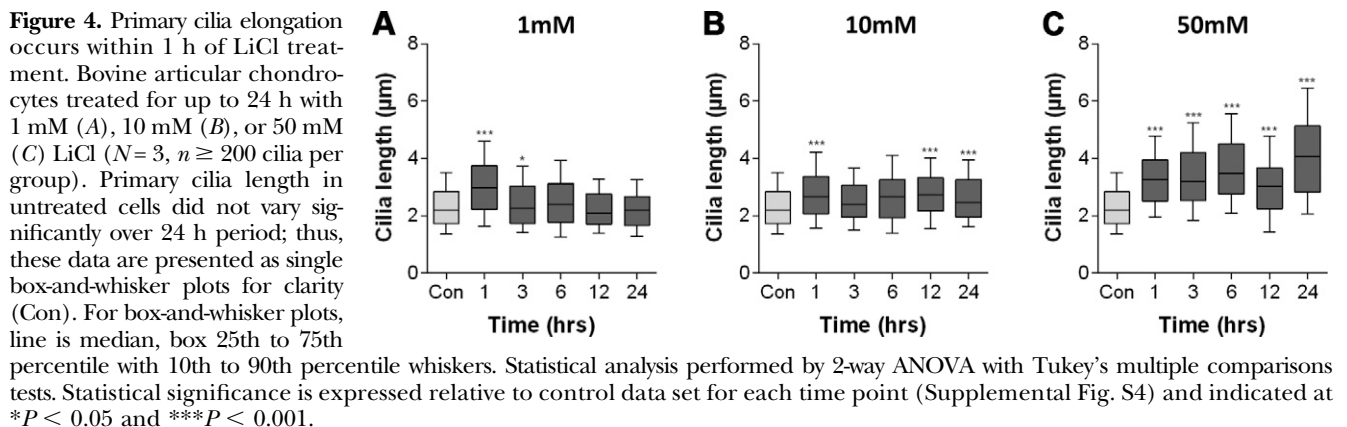
Figure 3. LiCl triggers primary cilia elongation independent of GSK inhibition and tubulin acetylation. *A*) Confocal immunofluorescence of bovine articular chondrocytes treated for 24 h with 50 mM LiCl. Primary cilia were labeled for acetylated α-tubulin (red), and nuclei were counterstained with DAPI (blue). Scale bars, 20 μm. White boxes indicate enlarged representative cells with acetylated tubulin image shown under each condition. Scale bars, 5 μm. *B*) Representative Western blot for acetylated tubulin (Acet Tub) and tubulin (Tub). *C*) Quantification of band intensity for tubulin Western blot analysis; tubulin acetylation is expressed relative to total tubulin ($N = 3$). *D*) Bovine articular chondrocytes were treated with 20 μm CHIR-99021 (CHIR) for 24 h. Scale bars, 5 μm. Primary cilia prevalence ($N = 3$, $n = 30$ fields per group) (*E*) and primary cilia length ($N = 3$, $n \geq 200$ cilia per group) (*F*) at 24 h. Data represent mean ± SD. For box-and-whisker plots, line is median, box 25th to 75th percentile with 10th to 90th percentile whiskers. Statistical analysis performed by 2-way ANOVA with Tukey's multiple comparisons tests. Statistical significance is expressed relative to untreated control.

phenomenon could be relevant for human patients. However, the physiologic dose of lithium in patients undergoing therapy is significantly lower than that used in the current *in vitro* study, ranging from 0.8 to 1.3 mmol/L. The effects of lithium on chondrocyte primary cilia length were therefore explored *in vivo* using a rat model. Primary cilia were labeled for acetylated α-tubulin (Fig. 6*C*), and primary cilia length was quantified through the depth of the articular cartilage. In rats receiving dietary lithium, primary cilia length was significantly increased relative to the control group from 1.44 ± 0.6 to 1.72 ± 0.6 μm, respectively, indicating that long-term treatment with physiologically relevant doses can influence primary cilia structure *in vivo* (Fig. 6*D*).

DISCUSSION

The current study demonstrated that LiCl induces primary cilia elongation in articular chondrocytes both *in vitro* and in an *in vivo* rat model. In the presence of LiCl, ligand-dependent Hedgehog signaling was significantly inhibited, directly correlating with these changes in cilia length. We suggest that this inhibition may be related to the reorganization of the ciliary compartment and dilution of Hedgehog signaling components such as Arl13b (Fig. 5*J*) within the axoneme. Mahjoub and Stearns (50) report that in cells exhibiting supernumerary centrioles, the multiciliated phenotype that arises inhibits Hedgehog signaling. Dilution of Hedgehog signaling components, such as

Figure 4. Primary cilia elongation occurs within 1 h of LiCl treatment. Bovine articular chondrocytes treated for up to 24 h with 1 mM (*A*), 10 mM (*B*), or 50 mM (*C*) LiCl ($N = 3$, $n \geq 200$ cilia per group). Primary cilia length in untreated cells did not vary significantly over 24 h period; thus, these data are presented as single box-and-whisker plots for clarity (Con). For box-and-whisker plots, line is median, box 25th to 75th percentile with 10th to 90th percentile whiskers. Statistical analysis performed by 2-way ANOVA with Tukey's multiple comparisons tests. Statistical significance is expressed relative to control data set for each time point (Supplemental Fig. S4) and indicated at *$P < 0.05$ and ***$P < 0.001$.
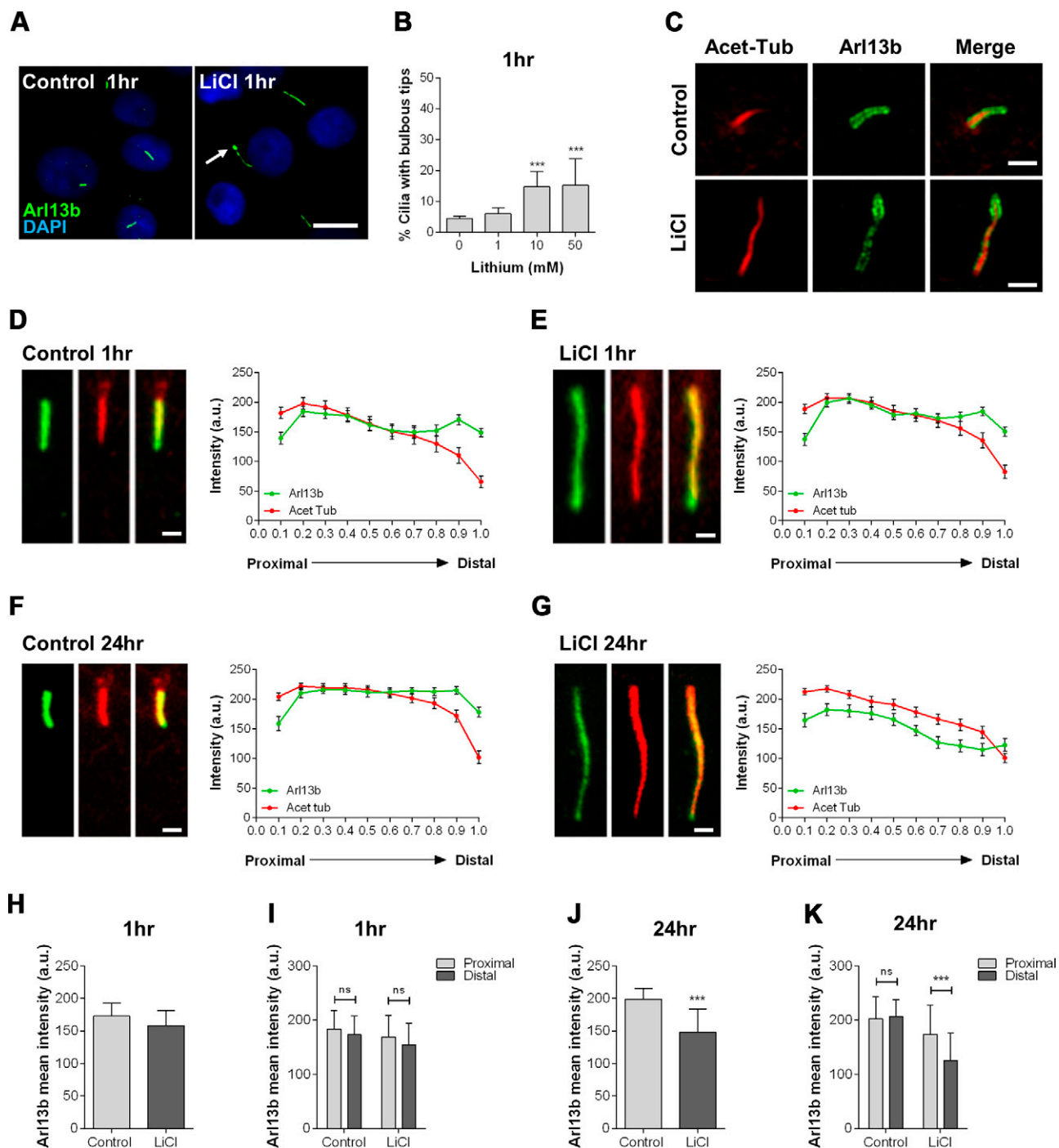
Figure 5. LiCl-induced primary cilia elongation is associated with reorganization of ciliary compartment. *A*) Immunofluorescence for Arl13b. Arrow identifies accumulation of protein forming bulb at ciliary tip observed at 1 h. Scale bar, 10 μm. *B*) Prevalence of cilia with bulbous tips after 1 h LiCl treatment ($N = 3$, $n = 15$ fields). *C*) Immunocytochemistry for acetylated α-tubulin (red) and Arl13b (green); bulbous tips were imaged after 1 h LiCl treatment (50 mM) using structured illumination microscopy. Data represent means ± SD. Distribution of acetylated α-tubulin (red) and Arl13b (green) staining within control cilia and LiCl-treated cilia at 1 h (*D, E*) and 24 h (*F, G*). Scale bars, 1 μm. Graphs show fluorescence intensity along axoneme from base (proximal) to tip (distal). Data represent means ± SEM ($N = 3$, $n = 30$ cilia per group). Mean Arl13b intensity within cilia at 1 h (*H*) and 24 h (*J*) ($N = 3$, $n = 30$ cilia). Mean Arl13b intensity in proximal and distal region of ciliary axoneme at 1 h (*I*) and 24 h (*K*) ($N = 3$, $n = 30$ cilia per group). Data represent means ± SD. Statistical analysis performed by 2-way ANOVA with Tukey's multiple comparisons tests. Statistical significance is expressed relative to untreated control unless otherwise shown and indicated at ***$P < 0.001$.

Arl13b and Smo, across multiple primary cilia reduces the amount of protein per micrometer in the axoneme and inhibits pathway activity (50), similar to what we observed for a single elongated cilium in the current study.

Mice lacking Arl13b exhibit abnormal Hedgehog signaling (31). In null mutants, Smo localizes exclusively to the ciliary compartment, and consequently Gli transcriptional activators are constitutively active, albeit at low levels

Figure 6. LiCl causes primary cilia elongation in isolated human chondrocytes and *in vivo* in rat chondrocytes. *A*) Immunofluorescence of isolated human articular chondrocytes treated for 24 h with LiCl (50 mM). Scale bars, 20 μm. White boxes indicate enlarged representative cells shown under each condition. Scale bars, 5 μm. Primary cilia were labeled for acetylated α-tubulin (red) and arl13b (green); nuclei were counterstained with DAPI (blue). *B*) Primary cilia length (*N* = 3, *n* ≥ 100 cilia per group) at 24 h. *C*) Immunohistochemistry of rat chondrocytes *in situ* having been exposed to dietary lithium for 9 mo. Scale bars, 2 μm. Primary cilia were labeled for acetylated α-tubulin (green); nuclei were counterstained with DAPI (blue). *D*) Primary cilia length was quantified throughout depth of tissue (*N* = 3, *n* ≥ 100 cilia per group). Data represent means ± SD. For box-and-whisker plots, line is median, box 25th to 75th percentile with 10th to 90th percentile whiskers. Statistical analysis performed by 2-way ANOVA with Tukey's multiple comparisons tests. Statistical significance is expressed relative to untreated control and indicated at ****P* < 0.001.
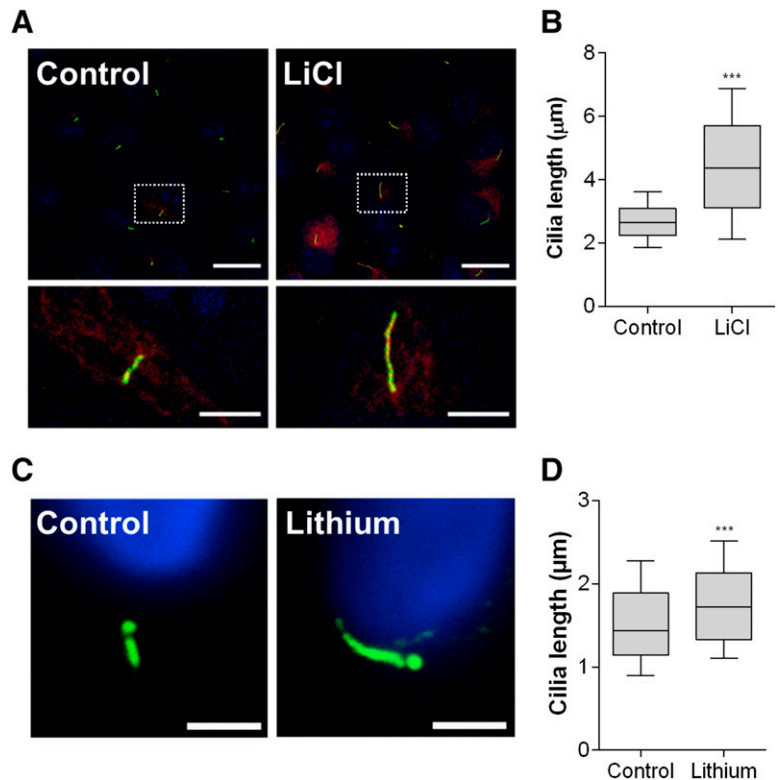
(31). In the absence of Arl13b, the enrichment of Gli proteins at the ciliary tip does not occur in response to ligand stimulation, and consequently the pathway cannot be further activated despite the constitutive ciliary localization of Smo (30). While we observed alterations in the ciliary localization of Arl13b after LiCl treatment, a lack of suitable antibodies coupled with the low expression of Hedgehog pathway components in adult chondrocytes precluded reliable quantification of Hedgehog signaling proteins within the ciliary compartment. However, we hypothesize that alterations to Arl13b trafficking and thus distribution within the cilium would similarly impact the dynamic localization of Smo and Gli proteins in response to Hedgehog ligand. However, several intraflagellar and ciliary proteins have been linked to the trafficking of Hedgehog proteins in addition to Arl13b, such as Kif3a (44, 51), Kif7 (52), Dync2h1 (53), Ift88 (44, 51), Ift80 (54), Ift25 (55), Ellis van Creveld protein and Ellis van Creveld protein 2 (56, 57), Gpr161 (58), and, more recently, adenylate cyclase 5 and 6 (59), the function of which could also be influenced by LiCl. Alternatively, however, Hedgehog inhibition could also result from the disruption of proteins at the ciliary tip, such as Kif7, which have previously been shown to regulate Gli protein activation (60, 61).

In contrast to previous reports (14, 47), our results indicate that in articular chondrocytes cilia elongation does not occur as a consequence of GSK inhibition (Fig. 3*D–F*). This finding is consistent with our observation that GSK inhibition does not inhibit Hedgehog signaling and supports our hypothesis that cilia elongation is of importance. In neuronal cells, LiCl induces primary cilia elongation through the inhibition of adenylate cyclase and a reduction in cAMP levels (15).

We have previously shown that modulation of cAMP influences cilia length in articular chondrocytes (62). Therefore, it is likely that LiCl acts in a similar manner to trigger cilia elongation in chondrocytes. However, the influence of cAMP on chondrocyte cilia structure is complex, as both adenylate cyclase inhibition and exogenous cAMP induce cilia elongation in isolated chondrocytes (62). Intriguingly, mechanical loading both modulates cAMP levels and influences primary cilia length in articular chondrocytes, highlighting the potential existence of a feedback mechanism to regulate ciliary signaling (46, 63). Indeed, changes in ciliary structure have been reported in mechanically compromised osteoarthritic cartilage such that the cilium elongates with increasing disease severity (64).

The accumulation of activated β-catenin in response to LiCl and subsequent activation of canonical Wnt signaling through the inhibition of GSKβ is well established. Zinke *et al.* (65) have suggested that β-catenin accumulation may sequester activated Gli proteins away from the nucleus in response to LiCl treatment in medulloblastoma cells. However, in the current study, we did not observe significant accumulation of activated β-catenin, and GSK inhibition alone did not inhibit Hedgehog signaling. It therefore seems unlikely that LiCl is functioning primarily as a GSK inhibitor in articular chondrocytes. Indeed, previous studies have shown that while GSK inhibition alone negatively affects cartilage health, resulting in increased cartilage degradation and susceptibility to injury (66), administration of dietary lithium does not lead to cartilage degradation (5, 6). Lancaster *et al.* (67) report that the cilium exerts a negative influence over canonical Wnt signaling by sequestering β-catenin away from the nucleus such that in the presence of cilia, LiCl cannot activate Wnt

signaling in mouse embryonic fibroblasts. Given that the majority of articular chondrocytes are ciliated, this may provide an explanation for the lack of β-catenin activation observed in the current study.

Both dietary and intra-articular injection of LiCl reduce cartilage degradation in the destabilization of medial meniscus model of OA while having no overt effects on cartilage health (5). Similarly, Hedgehog inhibition also reduces cartilage damage and slows disease progression in this model (10). More recent studies report that the classic Hedgehog pathway inhibitor cyclopamine attenuates *in vivo* inflammation and cartilage degradation in adjuvant-induced arthritis (68). Therefore, we suggest that in addition to its effects on inflammatory signaling, the efficacy of LiCl in destabilization of medial meniscus studies may also be linked to its influence over Hedgehog signaling.

Minashima *et al.* (5) report that LiCl inhibits NF-κB signaling in response to IL-1 treatment. Previously we have reported a role for the cilium in NF-κB signaling such that, in the absence of cilia, NF-κB signaling is both delayed and attenuated, a consequence of which is that chondrocytes are unable to up regulate nitric oxide and prostaglandin E_2 production in response to IL-1 (62, 69). Therefore, an intriguing possibility is that LiCl might also be influencing inflammatory signaling through the modulation of cilia length; however, this remains to be investigated.

That cilia elongation was observed both in human chondrocytes and chondrocytes *in vivo* after lithium administration highlights the potential of this drug as a treatment for cartilage disease in human patients. Although an association between rheumatoid arthritis and psychiatric disorders has been postulated (70), few studies have explored any association between OA and bipolar disorder. Recently it was reported that the incidence of OA in patients with bipolar disorder was increased (71); however, this was not found to be associated with the use of mood stabilizers, and it therefore remains to be investigated whether patients undergoing lithium therapy are protected against this disease. We suggest that targeting Hedgehog signaling through the modulation of primary cilia structure may provide a novel means by which to reduce cartilage degradation in OA. Importantly, the involvement of the cilium in this response facilitates a multifaceted approach to OA therapy, as it may enable the targeting of multiple pathophysiologic pathways through a single organelle. The study is therefore the first to indicate the potential of pharmaceutical ciliotherapy for the treatment of OA. [FJ]

REFERENCES

1. Williams, R. S., and Harwood, A. J. (2000) Lithium therapy and signal transduction. *Trends Pharmacol. Sci.* **21**, 61–64

2. Goodwin, F. K., and Ghaemi, S. N. (1999) The impact of the discovery of lithium on psychiatric thought and practice in the USA and Europe. *Aust. N. Z. J. Psychiatry* **33** (Suppl), S54–S64

3. Lenox, R. H., and Hahn, C. G. (2000) Overview of the mechanism of action of lithium in the brain: fifty-year update. *J. Clin. Psychiatry* **61** (Suppl 9), 5–15

4. Hui, W., Litherland, G. J., Jefferson, M., Barter, M. J., Elias, M. S., Cawston, T. E., Rowan, A. D., and Young, D. A. (2010) Lithium protects cartilage from cytokine-mediated degradation by reducing collagen-degrading MMP production *via* inhibition of the P38 mitogen-activated protein kinase pathway. *Rheumatology (Oxford)* **49**, 2043–2053

5. Minashima, T., Zhang, Y., Lee, Y., and Kirsch, T. (2014) Lithium protects against cartilage degradation in osteoarthritis. *Arthritis Rheumatol.* **66**, 1228–1236

6. Thompson, C. L., Yasmin, H., Varone, A., Wiles, A., Poole, C. A., and Knight, M. M. (2015) Lithium chloride prevents interleukin-1β induced cartilage degradation and loss of mechanical properties. *J. Orthop. Res.* **33**, 1552–1559

7. Peng, Z., Ji, Z., Mei, F., Lu, M., Ou, Y., and Cheng, X. (2013) Lithium inhibits tumorigenic potential of PDA cells through targeting Hedgehog-GLI signaling pathway. *PLoS One* **8**, e61457

8. Tchetina, E. V., Squires, G., and Poole, A. R. (2005) Increased type II collagen degradation and very early focal cartilage degeneration is associated with upregulation of chondrocyte differentiation related genes in early human articular cartilage lesions. *J. Rheumatol.* **32**, 876–886

9. Zhou, J., Chen, Q., Lanske, B., Fleming, B. C., Terek, R., Wei, X., Zhang, G., Wang, S., Li, K., and Wei, L. (2014) Disrupting the Indian hedgehog signaling pathway *in vivo* attenuates surgically induced osteoarthritis progression in Col2a1-CreERT2; Ihhfl/fl mice. *Arthritis Res. Ther.* **16**, R11

10. Lin, A. C., Seeto, B. L., Bartoszko, J. M., Khoury, M. A., Whetstone, H., Ho, L., Hsu, C., Ali, S. A., and Alman, B. A. (2009) Modulating Hedgehog signaling can attenuate the severity of osteoarthritis. *Nat. Med.* **15**, 1421–1425

11. Wei, F., Zhou, J., Wei, X., Zhang, J., Fleming, B. C., Terek, R., Pei, M., Chen, Q., Liu, T., and Wei, L. (2012) Activation of Indian hedgehog promotes chondrocyte hypertrophy and upregulation of MMP-13 in human osteoarthritic cartilage. *Osteoarthritis Cartilage* **20**, 755–763

12. Zhang, C., Wei, X., Chen, C., Cao, K., Li, Y., Jiao, Q., Ding, J., Zhou, J., Fleming, B. C., Chen, Q., Shang, X., and Wei, L. (2014) Indian hedgehog in synovial fluid is a novel marker for early cartilage lesions in human knee joint. *Int. J. Mol. Sci.* **15**, 7250–7265

13. Miyoshi, K., Kasahara, K., Miyazaki, I., and Asanuma, M. (2009) Lithium treatment elongates primary cilia in the mouse brain and in cultured cells. *Biochem. Biophys. Res. Commun.* **388**, 757–762

14. Nakakura, T., Asano-Hoshino, A., Suzuki, T., Arisawa, K., Tanaka, H., Sekino, Y., Kiuchi, Y., Kawai, K., and Hagiwara, H. (2015) The elongation of primary cilia *via* the acetylation of α-tubulin by the treatment with lithium chloride in human fibroblast KD cells. *Med. Mol. Morphol.* **48**, 44–53

15. Ou, Y., Ruan, Y., Cheng, M., Moser, J. J., Rattner, J. B., and van der Hoorn, F. A. (2009) Adenylate cyclase regulates elongation of mammalian primary cilia. *Exp. Cell Res.* **315**, 2802–2817

16. Nakamura, S., Takino, H., and Kojima, M. K. (1987) Effect of lithium on flagellar length in *Chlamydomonas reinhardtii*. *Cell Struct. Funct.* **12**, 369–374

17. Ross, A. J., May-Simera, H., Eichers, E. R., Kai, M., Hill, J., Jagger, D. J., Leitch, C. C., Chapple, J. P., Munro, P. M., Fisher, S., Tan, P. L., Phillips, H. M., Leroux, M. R., Henderson, D. J., Murdoch, J. N., Copp, A. J., Eliot, M. M., Lupski, J. R., Kemp, D. T., Dollfus, H., Tada, M., Katsanis, N., Forge, A., and Beales, P. L. (2005) Disruption of Bardet-Biedl syndrome ciliary proteins perturbs planar cell polarity in vertebrates. *Nat. Genet.* **37**, 1135–1140

18. Simons, M., Gloy, J., Ganner, A., Bullerkotte, A., Bashkurov, M., Krönig, C., Schermer, B., Benzing, T., Cabello, O. A., Jenny, A., Mlodzik, M., Polok, B., Driever, W., Obara, T., and Walz, G. (2005) Inversin, the gene product mutated in nephronophthisis type II, functions as a molecular switch between Wnt signaling pathways. *Nat. Genet.* **37**, 537–543

19. Haycraft, C. J., Banizs, B., Aydin-Son, Y., Zhang, Q., Michaud, E. J., and Yoder, B. K. (2005) Gli2 and Gli3 localize to cilia and require the intraflagellar transport protein polaris for processing and function. *PLoS Genet.* **1**, e53

20. Wann, A. K., Zuo, N., Haycraft, C. J., Jensen, C. G., Poole, C. A., McGlashan, S. R., and Knight, M. M. (2012) Primary cilia mediate mechanotransduction through control of ATP-induced Ca^{2+} signaling in compressed chondrocytes. *FASEB J.* **26**, 1663–1671

21. McGlashan, S. R., Haycraft, C. J., Jensen, C. G., Yoder, B. K., and Poole, C. A. (2007) Articular cartilage and growth plate defects are associated with chondrocyte cytoskeletal abnormalities in Tg737orpk mice lacking the primary cilia protein polaris. *Matrix Biol.* **26**, 234–246

22. Farnum, C. E., and Wilsman, N. J. (2011) Orientation of primary cilia of articular chondrocytes in three-dimensional space. *Anat. Rec. (Hoboken)* **294**, 533–549

23. Dishinger, J. F., Kee, H. L., Jenkins, P. M., Fan, S., Hurd, T. W., Hammond, J. W., Truong, Y. N., Margolis, B., Martens, J. R., and Verhey, K. J. (2010) Ciliary entry of the kinesin-2 motor KIF17 is regulated by importin-beta2 and RanGTP. *Nat. Cell Biol.* **12**, 703–710

24. Garcia-Gonzalo, F. R., Corbit, K. C., Sirerol-Piquer, M. S., Ramaswami, G., Otto, E. A., Noriega, T. R., Seol, A. D., Robinson, J. F., Bennett, C. L., Josifova, D. J., García-Verdugo, J. M., Katsanis, N., Hildebrandt, F., and Reiter, J. F. (2011) A transition zone complex regulates mammalian ciliogenesis and ciliary membrane composition. *Nat. Genet.* **43**, 776–784

25. Pedersen, L. B., and Rosenbaum, J. L. (2008) Intraflagellar transport (IFT) role in ciliary assembly, resorption and signalling. *Curr. Top. Dev. Biol.* **85**, 23–61

26. Kozminski, K. G., Johnson, K. A., Forscher, P., and Rosenbaum, J. L. (1993) A motility in the eukaryotic flagellum unrelated to flagellar beating. *Proc. Natl. Acad. Sci. USA* **90**, 5519–5523

27. Iomini, C., Babaev-Khaimov, V., Sassaroli, M., and Piperno, G. (2001) Protein particles in *Chlamydomonas flagella* undergo a transport cycle consisting of four phases. *J. Cell Biol.* **153**, 13–24

28. Pazour, G. J., Dickert, B. L., and Witman, G. B. (1999) The DHC1b (DHC2) isoform of cytoplasmic dynein is required for flagellar assembly. *J. Cell Biol.* **144**, 473–481

29. Marshall, W. F., and Rosenbaum, J. L. (2001) Intraflagellar transport balances continuous turnover of outer doublet microtubules: implications for flagellar length control. *J. Cell Biol.* **155**, 405–414

30. Larkins, C. E., Aviles, G. D., East, M. P., Kahn, R. A., and Caspary, T. (2011) Arl13b regulates ciliogenesis and the dynamic localization of Shh signaling proteins. *Mol. Biol. Cell* **22**, 4694–4703

31. Caspary, T., Larkins, C. E., and Anderson, K. V. (2007) The graded response to Sonic hedgehog depends on cilia architecture. *Dev. Cell* **12**, 767–778

32. Corbit, K. C., Aanstad, P., Singla, V., Norman, A. R., Stainier, D. Y., and Reiter, J. F. (2005) Vertebrate Smoothened functions at the primary cilium. *Nature* **437**, 1018–1021

33. Tukachinsky, H., Lopez, L. V., and Salic, A. (2010) A mechanism for vertebrate Hedgehog signaling: recruitment to cilia and dissociation of SuFu-Gli protein complexes. *J. Cell Biol.* **191**, 415–428

34. Kim, J., Kato, M., and Beachy, P. A. (2009) Gli2 trafficking links Hedgehog-dependent activation of Smoothened in the primary cilium to transcriptional activation in the nucleus. *Proc. Natl. Acad. Sci. USA* **106**, 21666–21671

35. Buttitta, L., Mo, R., Hui, C. C., and Fan, C. M. (2003) Interplays of Gli2 and Gli3 and their requirement in mediating Shh-dependent sclerotome induction. *Development* **130**, 6233–6243

36. Engel, B. D., Ludington, W. B., and Marshall, W. F. (2009) Intraflagellar transport particle size scales inversely with flagellar length: revisiting the balance-point length control model. *J. Cell Biol.* **187**, 81–89

37. Wren, K. N., Craft, J. M., Tritschler, D., Schauer, A., Patel, D. K., Smith, E. F., Porter, M. E., Kner, P., and Lechtreck, K. F. (2013) A differential cargo-loading model of ciliary length regulation by IFT. *Curr. Biol.* **23**, 2463–2471

38. Ludington, W. B., Wemmer, K. A., Lechtreck, K. F., Witman, G. B., and Marshall, W. F. (2013) Avalanche-like behavior in ciliary import. *Proc. Natl. Acad. Sci. USA* **110**, 3925–3930

39. Cruz, C., Ribes, V., Kutejova, E., Cayuso, J., Lawson, V., Norris, D., Stevens, J., Davey, M., Blight, K., Bangs, F., Mynett, A., Hirst, E., Chung, R., Balaskas, N., Brody, S. L., Marti, E., and Briscoe, J. (2010) Foxj1 regulates floor plate cilia architecture and modifies the response of cells to Sonic hedgehog signalling. *Development* **137**, 4271–4282

40. Chowdhury, T. T., Bader, D. L., and Lee, D. A. (2001) Dynamic compression inhibits the synthesis of nitric oxide and PGE(2) by IL-1beta-stimulated chondrocytes cultured in agarose constructs. *Biochem. Biophys. Res. Commun.* **285**, 1168–1174

41. Poole, C. A., Zhang, Z. J., and Ross, J. M. (2001) The differential distribution of acetylated and detyrosinated alpha-tubulin in the microtubular cytoskeleton and primary cilia of hyaline cartilage chondrocytes. *J. Anat.* **199**, 393–405

42. Larionov, A., Krause, A., and Miller, W. (2005) A standard curve based method for relative real time PCR data processing. *BMC Bioinformatics* **6**, 62

43. Klein, P. S., and Melton, D. A. (1996) A molecular mechanism for the effect of lithium on development. *Proc. Natl. Acad. Sci. USA* **93**, 8455–8459

44. Huangfu, D., Liu, A., Rakeman, A. S., Murcia, N. S., Niswander, L., and Anderson, K. V. (2003) Hedgehog signalling in the mouse requires intraflagellar transport proteins. *Nature* **426**, 83–87

45. Liu, A., Wang, B., and Niswander, L. A. (2005) Mouse intraflagellar transport proteins regulate both the activator and repressor functions of Gli transcription factors. *Development* **132**, 3103–3111

46. Thompson, C. L., Chapple, J. P., and Knight, M. M. (2014) Primary cilia disassembly down-regulates mechanosensitive Hedgehog signalling: a feedback mechanism controlling ADAMTS-5 expression in chondrocytes. *Osteoarthritis Cartilage* **22**, 490–498

47. Ou, Y., Zhang, Y., Cheng, M., Rattner, J. B., Dobrinski, I., and van der Hoorn, F. A. (2012) Targeting of CRMP-2 to the primary cilium is modulated by GSK-3β. *PLoS One* **7**, e48773

48. Iomini, C., Li, L., Esparza, J. M., and Dutcher, S. K. (2009) Retrograde intraflagellar transport mutants identify complex A proteins with multiple genetic interactions in Chlamydomonas reinhardtii. *Genetics* **183**, 885–896

49. Piperno, G., Siuda, E., Henderson, S., Segil, M., Vaananen, H., and Sassaroli, M. (1998) Distinct mutants of retrograde intraflagellar transport (IFT) share similar morphological and molecular defects. *J. Cell Biol.* **143**, 1591–1601

50. Mahjoub, M. R., and Stearns, T. (2012) Supernumerary centrosomes nucleate extra cilia and compromise primary cilium signaling. *Curr. Biol.* **22**, 1628–1634

51. Huangfu, D., and Anderson, K. V. (2005) Cilia and Hedgehog responsiveness in the mouse. *Proc. Natl. Acad. Sci. USA* **102**, 11325–11330

52. Liem, K. F., Jr., He, M., Ocbina, P. J., and Anderson, K. V. (2009) Mouse Kif7/Costal2 is a cilia-associated protein that regulates Sonic hedgehog signaling. *Proc. Natl. Acad. Sci. USA* **106**, 13377–13382

53. Ocbina, P. J., and Anderson, K. V. (2008) Intraflagellar transport, cilia, and mammalian Hedgehog signaling: analysis in mouse embryonic fibroblasts. *Dev. Dyn.* **237**, 2030–2038

54. Beales, P. L., Bland, E., Tobin, J. L., Bacchelli, C., Tuysuz, B., Hill, J., Rix, S., Pearson, C. G., Kai, M., Hartley, J., Johnson, C., Irving, M., Elcioglu, N., Winey, M., Tada, M., and Scambler, P. J. (2007) IFT80, which encodes a conserved intraflagellar transport protein, is mutated in Jeune asphyxiating thoracic dystrophy. *Nat. Genet.* **39**, 727–729

55. Keady, B. T., Samtani, R., Tobita, K., Tsuchya, M., San Agustin, J. T., Follit, J. A., Jonassen, J. A., Subramanian, R., Lo, C. W., and Pazour, G. J. (2012) IFT25 links the signal-dependent movement of Hedgehog components to intraflagellar transport. *Dev. Cell* **22**, 940–951

56. Ruiz-Perez, V. L., Blair, H. J., Rodriguez-Andres, M. E., Blanco, M. J., Wilson, A., Liu, Y. N., Miles, C., Peters, H., and Goodship, J. A. (2007) Evc is a positive mediator of Ihh-regulated bone growth that localises at the base of chondrocyte cilia. *Development* **134**, 2903–2912

57. Blair, H. J., Tompson, S., Liu, Y. N., Campbell, J., MacArthur, K., Ponting, C. P., Ruiz-Perez, V. L., and Goodship, J. A. (2011) Evc2 is a positive modulator of Hedgehog signalling that interacts with Evc at the cilia membrane and is also found in the nucleus. *BMC Biol.* **9**, 14

58. Mukhopadhyay, S., Wen, X., Ratti, N., Loktev, A., Rangell, L., Scales, S. J., and Jackson, P. K. (2013) The ciliary G-protein-coupled receptor Gpr161 negatively regulates the Sonic hedgehog pathway *via* cAMP signaling. *Cell* **152**, 210–223

59. Vuolo, L., Herrera, A., Torroba, B., Menendez, A., and Pons, S. (2015) Ciliary adenylyl cyclases control the Hedgehog pathway. *J. Cell Sci.* **128**, 2928–2937

60. Wen, X., Lai, C. K., Evangelista, M., Hongo, J. A., de Sauvage, F. J., and Scales, S. J. (2010) Kinetics of Hedgehog-dependent full-length Gli3 accumulation in primary cilia and subsequent degradation. *Mol. Cell. Biol.* **30**, 1910–1922

61. He, M., Subramanian, R., Bangs, F., Omelchenko, T., Liem, K. F., Jr., Kapoor, T. M., and Anderson, K. V. (2014) The kinesin-4 protein Kif7 regulates mammalian Hedgehog signalling by organizing the cilium tip compartment. *Nat. Cell Biol.* **16**, 663–672

62. Wann, A. K., and Knight, M. M. (2012) Primary cilia elongation in response to interleukin-1 mediates the inflammatory response. *Cell. Mol. Life Sci.* **69**, 2967–2977

63. McGlashan, S. R., Knight, M. M., Chowdhury, T. T., Joshi, P., Jensen, C. G., Kennedy, S., and Poole, C. A. (2010) Mechanical loading modulates chondrocyte primary cilia incidence and length. *Cell Biol. Int.* **34**, 441–446

64. McGlashan, S. R., Cluett, E. C., Jensen, C. G., and Poole, C. A. (2008) Primary cilia in osteoarthritic chondrocytes: from chondrons to clusters. *Dev. Dyn.* **237**, 2013–2020

65. Zinke, J., Schneider, F. T., Harter, P. N., Thom, S., Ziegler, N., Toftgård, R., Plate, K. H., and Liebner, S. (2015) β-Catenin–Gli1 interaction regulates proliferation and tumor growth in medulloblastoma. *Mol. Cancer* **14**, 17

66. Litherland, G. J., Hui, W., Elias, M. S., Wilkinson, D. J., Watson, S., Huesa, C., Young, D. A., and Rowan, A. D. (2014) Glycogen synthase kinase 3 inhibition stimulates human cartilage destruction and exacerbates murine osteoarthritis. *Arthritis Rheumatol.* **66**, 2175–2187

67. Lancaster, M. A., Schroth, J., and Gleeson, J. G. (2011) Subcellular spatial regulation of canonical Wnt signalling at the primary cilium. *Nat. Cell Biol.* **13**, 700–707

68. Li, R., Cai, L., Ding, J., Hu, C. M., Wu, T. N., and Hu, X. Y. (2015) Inhibition of Hedgehog signal pathway by cyclopamine attenuates inflammation and articular cartilage damage in rats with adjuvant-induced arthritis. *J. Pharm. Pharmacol.* **67**, 963–971

69. Wann, A. K., Chapple, J. P., and Knight, M. M. (2014) The primary cilium influences interleukin-1β-induced NFκB signalling by regulating IKK activity. *Cell. Signal.* **26**, 1735–1742

70. Hsu, C. C., Chen, S. C., Liu, C. J., Lu, T., Shen, C. C., Hu, Y. W., Yeh, C. M., Chen, P. M., Chen, T. J., and Hu, L. Y. (2014) Rheumatoid arthritis and the risk of bipolar disorder: a nationwide population-based study. *PLoS One* **9**, e107512

71. Forty, L., Ulanova, A., Jones, L., Jones, I., Gordon-Smith, K., Fraser, C., Farmer, A., McGuffin, P., Lewis, C. M., Hosang, G. M., Rivera, M., and Craddock, N. (2014) Comorbid medical illness in bipolar disorder. *Br. J. Psychiatry* **205**, 465–472